Stable *peri*-Xanthenoxanthene Thin-Film Transistors with Efficient Carrier Injection

Norihito Kobayashi,* Mari Sasaki, and Kazumasa Nomoto

Organic Electronics Research Laboratory, Advanced Materials Laboratories, Sony Corporation, Atsugi 243-0021, Japan

Received October 16, 2008. Revised Manuscript Received November 27, 2008

We have synthesized and characterized stable organic semiconductors, 3,9-diphenyl-*peri*-xanthenoxanthene (Ph-PXX) and its soluble derivative for organic thin-film transistors (OTFTs). A π-system is stabilized against oxidation by introduction of heteroatoms into the reactive sites in the π-system. This strategy for stabilization does not suffer from the conventional tradeoff between environmental stability and efficient carrier injection, which appears when OSCs with deeper highest occupied molecular orbitals (HOMOs) are applied. UV−vis spectra of an air-saturated solution of Ph-PXX were unchanged over 120 h, indicating that it has an environmental stability. A HOMO level of Ph-PXX molecule was estimated to be only 5.1 eV below vacuum level, achieving efficient carrier injection. In fact, OTFTs with Ph-PXX showed high apparent mobility over 0.4 $cm^2/(V\ s)$ without demonstrating nonlinear behavior of source-drain ohmic contacts and have been shown to be stable for 5 months under ambient conditions. In addition, the OTFTs showed great thermal stability at temperatures up to 150 °C in air. These characteristics have been also achieved with a solution-processed OTFT with a soluble 3,9-bis(*p*-propylphenyl)-*peri*-xanthenoxanthene (PrPh-PXX). These results show that molecular design with passivation of the reactive cites is useful to make stable molecules with efficient carrier injection.

Introduction

Organic semiconductors (OSCs) applied to flexible electronics utilizing organic thin-film transistors (OTFTs) have received increasing attention.[1−3] Significant efforts have been made to develop OSCs in which the chemical and physical properties can be controlled.[2,4] High carrier mobility, high on/off ratio, ohmic contact between metal electrodes and OSC, and small subthreshold swing (*S*) are generally required in order to utilize OSCs for electronics.[2c,3,5] The stability of OSCs and thin-films determine the resulting properties of integrated TFTs for practical applications. This is because OSC films are exposed to various solvents and high-temperature thermal stress during the integration process.[3] The properties of OTFTs strongly depend on the properties of the OSC materials themselves.

Utilization of extended π-systems is a promising strategy to enhance the overlap of molecular orbitals between neighboring molecules in the solid state and leads to high mobility. In the case of acenes, however, the problem is the chemical instability of the longer molecules, which is attributed to localization of the frontier orbitals on specific atoms.[1,2d,6] On the other hand, a molecular-design strategy to set the highest occupied molecular orbital (HOMO) level of the OSCs as deep as possible from the vacuum level has been recently used to achieve stability in air.[7] According to the conventional Mott−Schottky model, metal (source and drain electrodes; S/D)−semiconductor junctions are expected to be ohmic when the work function of the metal is close to the HOMO of the semiconductor, which is the case for the p-type semiconductor.[2c,8] Therefore, a stable (unstable) molecule with a deep (shallow) HOMO leads to a higher (lower) Schottky barrier, resulting high (low) contact resistance. Thus, this molecular-design strategy for developing a stable OSC with high ionization potential (IP) causes an energy barrier to form at the metal-semiconductor interface, disturbing carrier injection. This tradeoff is expected to be overcome for high performance OTFTs. Herein, we show a novel class of OSCs that have been developed on the basis of the following concepts in order to establish as high environmental stability as possible along with high field-effect mobility and ohmic contacts as low as possible. This

* To whom correspondence should be addressed. E-mail: Norihito.Kobayashi@jp.sony.com. Telephone: 81 46 226 3349. Fax: 81 46 226 2369.

(1) (a) Klauk, H. *Organic Electronics: Materials, Manufacturing and Applications*, 1st ed; Wiley-VCH: Weinheim, Germany, 2006. (b) Bao, Z; Locklin, J. *Organic Field-Effect Transistors*; CRC Press: Boca Raton, FL, 2007.

(2) (a) Horowitz, G. *Adv. Mater.* **1998**, *10*, 365. (b) Katz, H. E.; Bao, Z.; Gilat, S. *Acc. Chem. Res.* **2001**, *34*, 359. (c) Sirringhaus, H. *Adv. Mater.* **2005**, *17*, 2411. (d) Allard, S.; Forster, M.; Souharce, B.; Thiem, H.; Scherf, U. *Angew. Chem., Int. Ed.* **2008**, *47*, 4070.

(3) (a) Nomoto, K.; Hirai, N.; Yoneya, N.; Kawashima, N.; Noda, M.; Wada, M.; Kasahara, J. *IEEE Trans. Electron Devices* **2005**, *52*, 1519. (b) Yagi, I.; Hirai, N.; Miyamoto, Y.; Noda, M.; Imaoka, A.; Yoneya, N.; Nomoto, K; Kasahara, J.; Yumoto, A.; Urabe, T. *J. Soc. Inf. Disp.* **2008**, *16*, 15.

(4) (a) Takimiya, K.; Kunugi, Y.; Otsubo, T. *Chem. Lett.* **2007**, *36*, 578. (b) Payne, M. M.; Parkin, S. R.; Anthony, J. E.; Kuo, C.-C.; Jackson, T. N. *J. Am. Chem. Soc.* **2005**, *127*, 4986.

(5) Newman, C. R.; Frisbie, C. D.; da Silva Filho, D. A.; Bredas, J.-L.; Ewbank, P. C.; Mann, K. R. *Chem. Mater.* **2004**, *16*, 4436.

(6) (a) Bendikov, M.; Wudl, F.; Perepichka, D. F. *Chem. Rev.* **2004**, *104*, 4891. (b) Suresh, C. H.; Gadre, S. R. *J. Org. Chem.* **1999**, *64*, 2505.

(7) Locklin, J.; Ling, M. M.; Sung, A.; Roberts, M. E.; Bao, Z. *Adv. Mater.* **2006**, *18*, 2989.

(8) Kahn, A.; Koch, N.; Gao, W. *J. Polym. Sci., Part B: Polym. Phys.* **2003**, *41*, 2529.

10.1021/cm802826m CCC: $40.75
Published on Web 01/12/2009

may be achieved by the following: (i) extended π-systems are utilized for high carrier mobility, (ii) reaction-active sites in the extended π-systems are passivated by an introduction of heteroatoms and/or substituents at the peripheral of the molecule for stability, (iii) HOMOs are set to be close to the work function of the metal electrodes, leading to a low Schottky barrier.

Experimental Section

General Remarks. All chemical reagents were purchased from Sigma-Aldrich Japan, Wako Pure Chemical Industries, TCI, or Kanto Chemical Co. and were used as received. MW-100LM was purchased from Sanwa Chemical Co., Japan.

Materials. *3,9-Dibromo*-peri-*xanthenoxanthene (Br-PXX).* To a stirred suspension of PXX[9] (5.0 g, 17.7 mmol) in anhydrous dichloromethane (460 mL) at −78 °C under an argon atmosphere was added a dichloromethane solution of bromine (5.5 g) over a period of 30 min. The brown solution was stirred for 1 h and warmed to room temperature, and stirred for 2 h. The reaction mixture was poured into a saturated aqueous solution of $NaHSO_3$, and stirred for 1 h. The mixture was filtered and washed with water, ethanol, and dichloromethane, yielding a yellow powder. The product was used in the next reaction without further purification: MS (MALDI-TOF) *m/z* 438 (M^+). ^{1}H NMR (400 MHz, C_4D_8O) δ 6.846−6.867 (*d*, J = 8.3 Hz, 2H), 7.330−7.353 (*d*, J = 9.3 Hz, 2H), 7.625−7.646 (*d*, J = 8.3 Hz, 2H), 7.825−7.848 (*d*, J = 9.3 Hz, 2H).

3,9-Diphenyl-peri-*xanthenoxanthen (Ph-PXX).* An aqueous solution of Na_2CO_3 (1 M, 40 mL) was added to the suspension of Br-PXX (7.46 g, 17.0 mmol) and (4,4,5,5-Tetramethyl-1,3,2-dioxaborolan-2-yl)benzene (10.4 g, 50.0 mmol) in toluene (200 mL). The mixture was degassed and purged with Ar for 30 min. Tetrakis(triphenylphophine)palladium(0) (2.4 g, 2.1 mmol) was added, and the system was degassed again. The mixture was refluxed for 3 days and allowed to cool to room temperature. The reaction mixture was poured into methanol (300 mL). The precipitate was filtered and washed with 20% HCl, water, and methanol (5.8 g). The residue was sublimed under high vacuum over a three-zone furnace, following extraction with THF using a Soxhlet extractor to give 3,9-diphenyl-*peri*-xanthenoxanthen as yellow crystals. ^{1}H NMR (400 MHz, C_4D_8O) δ 6.936−6.955 (*d*, J = 7.8 Hz, 2H), 7.132−7.135 (*d*, J = 9.3 Hz, 2H), 7.256−7.277 (*d*, J = 8.3 Hz, 2H), 7.544−7.565 (*d*, J = 6.3 Hz, 2H), 7.615−7.644 (*m*, 10H); MS (MALDI-TOF) *m/z* 434 (M^+). Anal. Calcd for $C_{32}H_{18}O_2$: C, 88.46; H, 4.18%. Found: C, 88.34; H, 3.96%.

*3,9-Bis(*p-*propylphenyl)*-peri-*xanthenoxanthene (PrPh-PXX).* PrPh-PXX was synthesized by utilizing the same procedure as that for Ph-PXX using *p*-propylphenyl boronic acid (8.20 g, 50.0 mmol) instead of (4,4,5,5-Tetramethyl-1,3,2-dioxaborolan-2-yl)benzene. ^{1}H NMR (400 MHz, C_4D_8O) δ 1.15−1.186 (*t*, J = 14.6 Hz, 6H), 1.835−1.873 (*m*, 4H), 2.813−2.850 (*m*, 4H), 6.904−6.923 (*d*, J = 8.3 Hz, 2H), 7.101−7.125 (*d*, J = 9.8 Hz, 2H), 7.228−7.248 (*d*, J = 8.3 Hz, 2H), 7.446−7.465 (*d*, J = 8.3 Hz, 4H), 7.505−7.526 (*d*, J = 8.3 Hz, 4H), 7.624−7.648 (*d*, J = 10.0 Hz, 2H); MS (MALDI-TOF) *m/z* 519 (M^+). Anal. Calcd for $C_{38}H_{30}O_2$: C, 88.00; H, 5.83%. Found: C, 87.88; H, 5.76%.

Instrumentation. ^{1}H NMR spectra were recorded on a JEOL JNM-AL400 FT/NMR system. Chemical shifts (δ) were reported in parts per million and TMS was used as an internal standard. MALDI-TOF-MS spectra were obtained on a Bruker Daltonics autoflex spectrometer. Elemental Analysis was performed using a Perkin-Elmer Instruments 2400 Series II CHNS/O analyzer. UV−vis spectra in 1,2,4-trichlorobenzene were recorded on a JASCO V-570 spectrometer. The cyclic voltammograms (CVs) were recorded on an ALS/CH Instruments Electrochemical Analyzer Model 650A. Molecular orbital calculations were carried out by density functional theory (DFT) methods at the B3LYP-6−31G(d,p) level using the Gaussian 03 program. The X-ray single crystal structure analysis was carried out on a Bruker AXS SMART APEX II diffractometer system. Crystal data and refinement details were summarized in the Supporting Information. The thermogravimetric analysis (TGA) was performed by a TA Instruments Q500. The differential scanning calorimetry (DSC) was carried out on a Seiko Instruments, Inc. DSC 6200. Out-of-plane XRDs were obtained with a RIGAKU ATX-G diffractometer. A Veeco Nanoscope IV equipped with Dimension 3100 was operated in tapping mode for AFM images.

Scheme 1. Molecular Structures of Anthanthrene and PXX

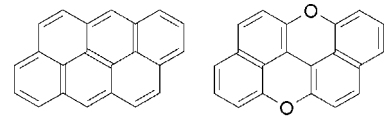

FET Device Fabrication and Evaluations. Top contact devices were made as follows; a solution containing 6.7 g of poly(4-vinylphenol), 10 g of cross-linking reagent (MW-100LM) and one drop of chlorosilane compounds in 70 mL of propyleneglycol monomethyl ether acetate (PGMEA) was spin-coated at 3000 rpm for 20 s on an *p*-doped silicon substrate, which functioned as the gate electrode. This PVP film was cured by heating at 150 °C for 20 min to give ca. 400 nm of PVP gate dielectric. OSCs were deposited at a rate of 0.7−1.0 Å/s under a pressure of 2×10^{-4} Pa to a final thickness of 50 nm as determined by a quartz crystal monitor. 1,2,3,4-Tetrahydronaphthalene solution of PrPh-PXX was spin-coated on the PVP gate dielectric and cured at 120 °C for 30 min. Shadow mask with L (channel length) = 50 μm and W (channel width) = 30 000 or 8000 μm were used after fabrication of OSCs to deposit the gold S/D electrodes. TFT measurements were performed in air using a Hewlett-Packard 4142B semiconductor parameter analyzer. The field-effect mobility (μ_{sat}) was calculated in the saturation regime of the I_d using the equation, $I_d = (WC_i/2L)(\mu_{sat.})(V_g - V_{th})$,[2] where C_i is the capacitance of the insulator, V_g and V_{th} are the gate and threshold voltages, respectively.

Results and Discussion

We have focused on anthanthrene as an extended π-system (Scheme 1). Oxygen atoms were introduced at the 6,12-positions to stabilize the π-system, which results in *peri*-xanthenoxanthene (6,12-dioxaanthanthrene, PXX). The shallow HOMO of PXX compared with anthanthrene was suggested by the DFT calculations. CV of PXX showed reversible redox peaks at $E^{1/2} = +0.34$ V against ferrocenium/ferrocene (Fc^+/Fc). Under the premise that the energy level of Fc^+/Fc is 4.8 eV below the vacuum level, the HOMO level of PXX was estimated to be ca. 5.1 eV.[10] In terms of the crystal structure, PXX is known to form a one-dimensional (1-D) stacking structure in a face-to-face manner.[9] This type of molecular arrangement is predicted to form stronger electronic coupling between molecules than the

(9) Asari, T.; Kobayashi, N.; Naito, T.; Inabe, T. *Bull. Chem. Soc. Jpn.* **2001**, *74*, 53.

(10) Pommerehne, J.; Vestweber, H.; Guss, W.; Mahrt, R. F.; Bässler, H.; Porsch, M.; Daub, J. *Adv. Mater.* **1995**, *7*, 551.

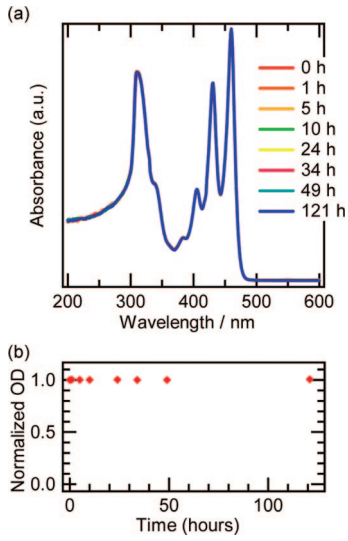

Figure 1. (a) UV−vis spectra of the 1,2,4-trichlorobenzene solution of Ph-PXX under air-bubbling. All curves were overlapped. (b) Time dependence of the optical density (OD) monitored at 460 nm.

Scheme 2. Synthetic Scheme to Obtain PXX Derivatives from PXX

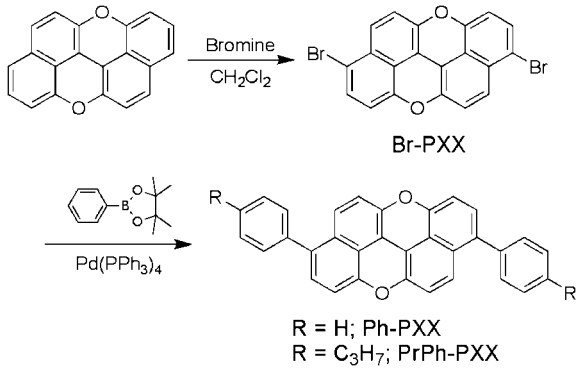

herringbone arrangement in polycyclic aromatic hydrocarbons.[11,12] Unfortunately, it is difficult for unsubstituted PXX to form a highly ordered thin film, because many single crystals are grown on the surface of the substrate from the solution or gas phase. This is a disadvantage for TFT applications. Thus, we have designed a phenyl-substituted derivative of 3,9-diphenyl-*peri*-xanthenoxanthene (Ph-PXX). Ph-PXX was synthesized from 3,9-dibromo-*peri*-xanthenoxanthene (Br-PXX) by a Suzuki-Miyaura coupling reaction with phenyl boronic acid pinacol ester (Scheme 2). PXX was predicted as less-reactive molecule using molecular orbital calculations. Because the stable PXX was reacted with bromine to obtain the starting material of Br-PXX, the more rigid chemical stability is expected to be realized upon transforming the remaining active sites of PXX into the substituents. CV of Ph-PXX showed reversible redox peaks at $E^{1/2} = +0.31$ V against Fc^+/Fc, and the HOMO was estimated to be ca. 5.1 eV. The comparable HOMO with PXX was achieved despite introduction of a phenyl group. In addition, the work function of Au was located at a similar energy level.[8] DFT calculations also supported this estimation. The calculated IP and the HOMO−LUMO (LUMO: lowest unoccupied molecular orbital) gap of Ph-PXX were 5.96 and 3.24 eV, respectively. The calculated IP of pentacene using the same methods was determined to be 5.94 eV. Therefore, just as the pentacene/Au provides a suitable interface for a low-resistance contact, Ph-PXX is also expected to ensure efficient carrier injection from metal electrodes such as Au and Ni, which are the most commonly used materials.

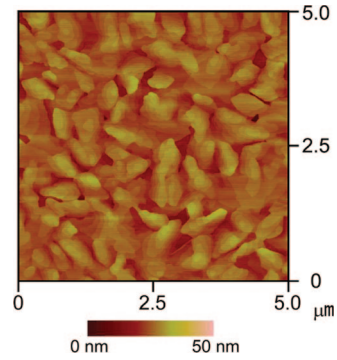

Figure 2. AFM image of the Ph-PXX film on PVP; rms roughness = 3.4 nm.

As shown in Figure 1, all UV−vis spectra for the air-saturated solution of Ph-PXX were not changed for over 120 h, suggesting chemical stability of the molecule. This stability could be attributed to the passivation effect of oxygen in the PXX backbone from an oxygen attack in the air. The optical HOMO−LUMO gap estimated from the absorption edge was 2.7 eV (Figure 1a). Note that pentacene, which has a similar HOMO to Ph-PXX, is unstable under similar experimental conditions and shows the most rapid decay in several hours.[13] Pentacene degraded in the presence of light and air, resulting in generation of byproducts of endoperoxide formation and/or dimerization. The sublimation point of the Ph-PXX crystals was determined to be around 300 °C by TGA, and no phase transition or melting point was observed by a DSC at temperatures lower than the sublimation point. Single-crystal X-ray diffraction analysis revealed the molecular structure of Ph-PXX and a face-to-face π-stacking arrangement of the molecules along the *c* axis with 3.45 Å spacing between neighboring molecules. The *d*-space value was obtained to be 18.2 Å by the out-of-plane XRD measurement of a deposited film on a Si substrate with the SiO_2 surface. Because it was consistent with the *b* axis of the single crystal, the molecular long axis of Ph-PXX is thought to be arranged perpendicular to the substrate in the thin film. These results indicate that although the HOMO was sufficient to allow an efficient hole-injection, Ph-PXX realized both chemical stability of the molecule and thermal stability in the crystal state as a molecular assembly. Additionally, a 1D face-to-face stacking structure was constructed. The molecular arrangement is favorable for a carrier transport.

Ph-PXX was vacuum-deposited on the highly doped Si substrate with a PVP gate dielectric.[14] Unlike in the case of PXX, a uniform and flat film was obtained without any three

(11) Deng, W. Q.; Goddard III, W. A. *J. Phys. Chem. B* **2004**, *108*, 8614.
(12) Kobayashi, K.; Masu, H.; Shuto, A.; Yamaguchi, K. *Chem. Mater.* **2005**, *17*, 6666.
(13) Maliakal, A.; Raghavachari, K.; Katz, H.; Chandross, E.; Siegrist, T. *Chem. Mater.* **2004**, *16*, 4980.

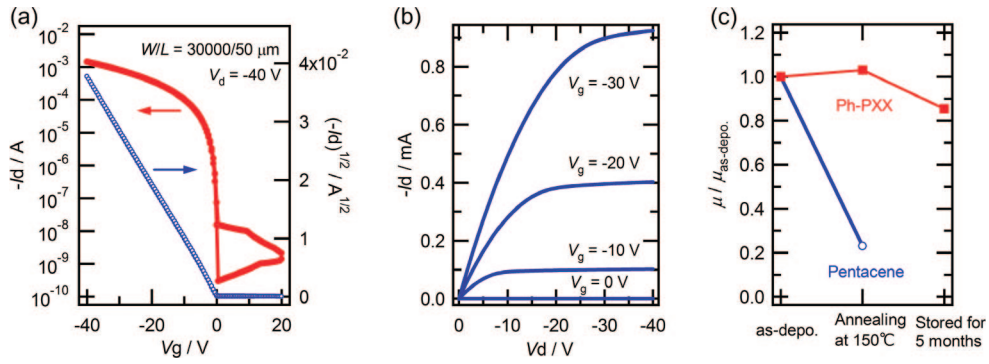

Figure 3. (a) Transfer and (b) output characteristics of the Ph-PXX TFT fabricated on a PVP gate insulator. (c) Thermal treatment and storage test for TFTs with Ph-PXX (red) and pentacene (blue).

Table 1. Field-Effect Mobilities (μ_{sat}) and Subthreshold Swings (S) of TFTs with PXX Derivatives

OSC	fabrication method[a]	thermal stress	μ_{sat} (cm^2/(V s))	S (V/dec)
Ph-PXX	VD	as-deposition	0.39−0.44	0.40−0.53
	VD	150 °C, 15 min	0.43−0.46	0.33−0.59
PrPh-PXX	SP	as-deposition	0.40−0.43	2.1−2.5
	VD	as-deposition	0.69−0.81	0.84−3.3

[a] VD = vacuum deposition; SP = solution process.

dimensionally randomly oriented crystal growth (Figure 2). The phenyl group appeared to affect the morphology of the thin-film. The top-contact TFT device showed typical p-channel field-effect characteristics without any hysterisis (Figure 3a). The ohmic characteristic in the linear region of the output characteristics (Figure 3b) ensures efficient carrier injection with low contact resistance between metal electrodes and the OSC film. The field-effect mobility in the saturation region (μ_{sat}) was estimated to be 0.39−0.44 cm^2/(V s), V_{th} was 0 V, and S was 0.40−0.53 V/decade (Table 1), which ensure the low voltage drive of the transistor. A thermal-treatment test was performed in order to check the thermal-resistance of TFTs. After annealing at 150 °C for 15 min, we observed a slight increase in the mobility, μ_{sat} = 0.43−0.46 cm^2/(V s), and a negligible shift in V_{th}. The ohmic characteristic was maintained even after annealing. The pentacene transistor, on the other hand, showed a drastic reduction for μ_{sat} (Figure 3c). Furthermore, a V_{th} shift of + 3 V was observed after annealing. Under ambient conditions, hysteresis, and V_{th} and off current of the annealed device maintained for five months, and the μ_{sat} showed only 15% degradation (Figure 3c). These results indicate that, by using Ph-PXX, we could provide the solution to overcome the tradeoff of OTFTs between environmental stability caused by the chemical stability of OSCs and contact problems from the HOMO of the molecule.

Other stable PXX derivatives can be designed with additional chemical and physical properties by changing the coupling reagents. Therefore, 3,9-bis(*p*-propylphenyl)-*peri*-xanthenoxanthene (PrPh-PXX) was synthesized to demonstrate the chemical property control (Scheme 2). The HOMO was determined to be consistent with that of Ph-PXX by CV estimation ($E^{1/2}$ = + 0.31 V against Fc^+/Fc), and the substituents do not significantly affect the

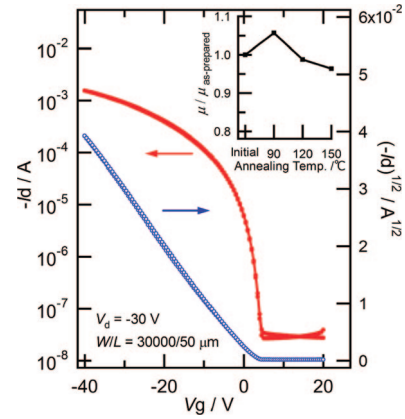

Figure 4. Transfer characteristics of the PrPh-PXX TFT fabricated on a PVP by spin-coating. (Inset) Trend in mobility by annealing.

HOMO. A *p*-propylphenyl group provided solubility in common organic solvents into a PXX-derivative and made it possible to adapt to a solution-process for TFT fabrication. 1,2,3,4-Tetrahydronaphthalene solution of PrPh-PXX was spin-coated on a PVP gate dielectric and cured in the air. The mobilities, μ_{sat}, of top-contact TFTs were estimated to be 0.40−0.43 cm^2/(V s). A repeated thermal stress test was performed as follows; each TFT was repeatedly annealed in the air for 15 min at 90, 120, and 150 °C in this order, and TFT characteristics were measured after each annealing. The devices showed mobility of 0.38−0.41 cm^2/Vs even after annealing at 150 °C (Figure 4). The solution-processed TFTs with PrPh-PXX were also environmentally and thermally stable. On the other hand, a thin-film of PrPh-PXX could be fabricated by a vacuum-deposition method. The mobilities, μ_{sat}, of TFTs fabricated by vacuum-deposition were estimated to be 0.69 − 0.81 cm^2/(V s). Therefore, it was shown that the PXX backbone has potential to establish a high carrier-mobility.

Conclusion

Ph-PXX and PrPh-PXX were synthesized and characterized as concrete examples of stable OSCs for OTFTs in which a π-system was stabilized against oxidation by introduction of heteroatoms and phenyl groups into the reactive sites in the π-system. This strategy for stabilization does not suffer from the conventional tradeoff between

(14) Yoneya, N.; Kimura, N.; Hirai, N.; Yagi, I.; Noda, M.; Nomoto, K.; Wada, M.; Kasahara, J. *SID Symp. Dig. Tech. Pap.* **2006**, *37*, 123.

environmental stability and efficient carrier injection, which appears when OSCs with deeper HOMOs are applied. OTFTs with Ph-PXX have shown high apparent mobility over 0.4 $cm^2/(V\ s)$ without demonstrating nonlinear behavior of S/D ohmic contacts, and have been shown to be stable for 5 months under ambient conditions. In addition, the OTFTs showed great thermal stability at temperatures up to 150 °C in air, which is important for integration of the OTFTs. These characteristics have been also achieved with a solution-processed OTFT with a soluble PrPh-PXX. PXX-derivatives are expected to expand the range of the device fabrication process toward flexible electronics.

Supporting Information Available: Results of the unsubstituted PXX deposition (Figure S1), ^1H NMR spectra (Figures S2−S4), DFT calculations (Figure S5), charts of CVs (Figure S6), TGA and DSC data (Figure S7), X-ray data (Figure S8−S9 and CIF), out-of-plane XRD (Figure S10), TFT characteristics (Figures S11−S13) (PDF); crystallographic information in CIF format. This material is available free of charge via the Internet at http://pubs.acs.org.

CM802826M